Supporting Information

A novel deep-blue fluorescent emitter employed as an identical exciplex acceptor for solution-processed multi-color OLEDs

Jie Pan,[a] Shiyue Zhang,[a] Zhongxin Zhou,[a] Yongtao Zhao,[a]
Shujing Jin,[a] Yanju Luo,[b*] Weiguo Zhu,[a*] and Yu Liu [a*]

[a]*School of Materials Science and Engineering, Jiangsu Collaboration Innovation Center of Photovoltaic Science and Engineering, Jiangsu Engineering Laboratory of Light-Electricity-Heat Energy-Converting Materials and Applications, Changzhou University, Changzhou 213164, (P. R. China)*

[b]*Analytical & Testing Centre, Sichuan University, Chengdu 610064, (P. R. China)*

luoyanju@scu.edu.cn (Y. Luo)
zhuwg18@126.com (W. Zhu);
liuyu03b@126.com (Y. Liu)

Contents

1. Materials and Measurements

All raw chemical materials are commercial from Energy Chemical Company Ltd and Bide Chemical Company Ltd. All reactions were carried out under N_2 atmosphere. ^1H and ^{13}C NMR spectra: All compounds were characterized by ^1H-NMR and ^{13}C-NMR using Bruker Dex-300/400/500 NMR, in which tetramethylsilane (TMS) was used as internal standard and deuterium chloroform (δ 7.26 ppm in ^1H NMR, δ 77.16 ppm in ^{13}C NMR) or deuterium dichloromethane (δ 5.30 ppm in ^1H NMR, δ 53.84 ppm in ^{13}C NMR) as solvent. Time-of-flight mass spectrometry (MS) were analyzed by mass spectrometry using the Bruker Autoflex MALDI-TOF instrument.

The single crystal structure of the target compound and its experimental data were confirmed by the Bruker APEX-II CCD X-ray single crystal diffractometer. Radiation tests were performed using MoKα (λ= 0.71073), data were processed by SADABS and SAINT, and molecular accumulation was obtained by SHELXL-2014.

The temperature rise rate of the target compound was controlled at 20 °C/min by NETZSCH STA449 from 25 °C to 400 °C.

The Gaussian 09 software is used to calculate the density functional theory of target molecules, in which the B3LYP/6-31G(d) unit is used to calculate the electron cloud distribution and corresponding energy levels.

UV-visible absorption spectra were recorded on a Shimadzu UV-2600. Steady-state and transient-state PL spectra, photoluminescence quantum yield (PLQY) and lifetime were carried out by using an Edinburgh FLS1000 Photoluminescence Spectrometer.

2. Computational method

The geometry of the ground state (S_0) was optimized at density functional theory (DFT) level using B3LYP hybrid functional and def2-SVP basis. The geometry of the lowest triplet state (T_1) was optimized using spin-unrestricted CAM-B3LYP hybrid functional and def2-SVP basis. The calculations described above were performed using Gaussian 09 software package the solvent effect in all the calculations was conducted using the polarizable continuum model (toluene).

3. Device fabrication and Measurement

Herein, poly(3,4-ethylenedioxythiophene)poly(styrene sulfonate) (PEDOT:PSS), 1,3,5-tri(m-pyrid-3-yl-phenyl)benzene (TmPyPB) and LiF function are employed as the hole injection, electron transporting layers, and electron injection, respectively. The emitting layer (EML) is exciplex with different donors and acceptor contents. The pre-patterned ITO substrates were cleaned with isopropyl alcohol, acetone, detergent and deionized water in an ultrasonic bath. Afterward, the substrates were dried in the oven at 80 °C. After UV-ozone treatment for 15 min, the PEDOT:PSS layer was directly spin-coated on the ITO substrate as the hole-injecting layer, and then the substrate was transferred into the glovebox filled with N_2 and annealed at 150 °C for 15 min. Then, The emissive layer was also prepared by spin-coating directly on the hole-transporting layer. Finally, TmPyPB as the electron-transporting material, LiF as the electron-injecting material and aluminium as the cathode material were consecutively thermally evaporated onto the emissive layer in a vacuum chamber of 1×10^{-4} Pa.

All device characterization steps after encapsulation were performed under ambient laboratory conditions at room temperature. The EL spectra and current density (J)-voltage (V)-Radiance (R) curves are obtained using a PHOTO RESEARCH Spectra Scan PR 735 photometer and a KEITHLEY 2400 Source Meter constant current source. The EQE values are done from the radiance, current density, and EL spectrum on the premise of a Lambertian distribution.

4. Ultraviolet photoelectron spectroscopy

To gain the energy levels of BOBTFB, BOBTFB:TCTA, BOBTFB:TAPC, and BOBTFB:m-MTDATA, ultraviolet photoelectron spectroscopy (UPS) was executed for the precise quantification of the highest occupied molecular orbital (HOMO) energy level of the neat film deposited onto an indium tin oxide (ITO) substrate. The high-energy and low-energy edges of the BOBTFB film and the films doped with different concentration ratios BOBTFB:TCTA(2:8), BOBTFB:TAPC (9:1), and BOBTFB:m-MTDATA (1:9) were measured by UPS spectra (Fig.S12). The dashed red lines mark the tangents of the curve, and the intersections of the tangents with the baseline give the edges of the UPS spectra from which the UPS width is determined, which is named

the kinetic energy difference (ΔE). Using the formula of $E_{\mathrm{HOMO,UPS}} = \Delta E - E_{\mathrm{He\text{-}I}}$(the photon energy of the He-I radiation, 21.22 eV), the $E_{\mathrm{HOMO,UPS}}$ value is calculated to be -5.92, -5.63, -5.57 and -5.52 eV for the films of BOBTFB, BOBTFB:TCTA(2:8), BOBTFB:TAPC (9:1), and BOBTFB:m-MTDATA (1:9). The LUMO energy level is evaluated to be -2.75, -2.61, -2.57 and -2.53 eV, respectively (Table S1).

5. Calculation of the k_{ISC} and k_{RISC}

$$\Phi_{ISC} = \frac{k_{ISC}}{k_p} \quad \text{(S1)}$$

$$\Phi_{RISC} = \frac{\Phi_d}{\Phi_{ISC}(\Phi_P + \Phi_d)} \quad \text{(S2)}$$

These calculations of key kinetic parameters were carried out by the following equations:

$$k_p = \frac{1}{\tau_p} \quad \text{(S3)}$$

$$k_d = \frac{1}{\tau_d} \quad \text{(S4)}$$

$$k_r = \frac{\Phi_p}{\tau_p} \quad \text{(S5)}$$

$$k_{ISC} = k_p(1 - \Phi_p) \quad \text{(S6)}$$

$$k_{TADF} = \frac{\Phi_d}{\Phi_{ISC}\tau_d} \quad \text{(S7)}$$

$$k_{RISC} = \frac{k_d k_p \Phi_d}{k_{ISC}\Phi_F} \quad \text{(S8)}$$

$$k_{nr}^{T} = k_d - \left(1 - \frac{k_{ISC}}{k_F + k_{ISC}}\right)k_{ISC} \quad \text{(S9)}$$

Where, Φ_p and Φ_d are the quantum efficiencies of prompt and delayed fluorescence; Φ_{ISC} is the efficiency of ISC process; k_p, k_d, k_{ISC}, k_r, k_{TADF}, $k_{nr}^{T}$and k_{RISC} are rate constants of prompt fluorescence, fluorescence decay, ISC process from S_1 toT_1 state, delayed fluorescence decay, nonradiative decay rate constant of T_1, and RISC process, respectively.

$$k_{\mathrm{RISC}}=\frac{\Phi_{DF}}{\Phi_{PF}}=\frac{\dfrac{A_2\tau_{DF}}{A_1\tau_{PF}+A_2\tau_{DF}}\Phi_T}{\dfrac{A_1\tau_{PF}}{A_1\tau_{PF}+A_2\tau_{DF}}\Phi_T}=\frac{k_{PF}k_{DF}\varphi_{DF}}{k_{ISC}\ \varphi_{PF}} \quad \text{(S10)}$$

$$k_{\mathrm{RISC}}=\mathrm{A}\exp\left(\frac{-\Delta E_{ST}}{k_BT}\right) \quad \text{(S11)}$$

where k_{PF}, k_{DF}, and k_{ISC} represent the rates of prompt fluorescence decay, delayed fluorescence decay, and singlet intersystem crossing (ISC), respectively. Φ_{T} is the total Φ_{PL}. Φ_{PF} and Φ_{DF} stand for the prompt and delayed components of PLQY, while τ_{PF} and τ_{DF} are the proportions of prompt and delayed fluorescence components of PL decay curves, respectively. k_{B} refers to the Boltzmann constant, and T is the temperature.

6. Chemical Synthesis

All reagents used in the experiments were purchased from commercial sources without further purification. For column chromatography, silica gel with 200-300 mesh was used.

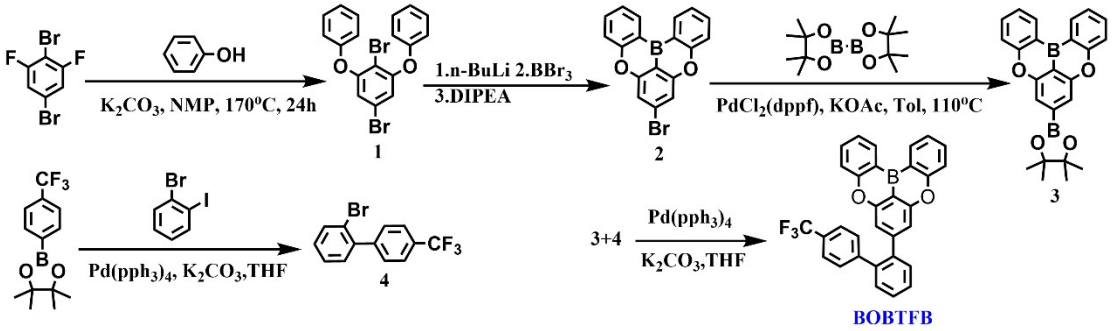

Scheme 1. Synthetic routes of the BOBTFB.

Compound 1:

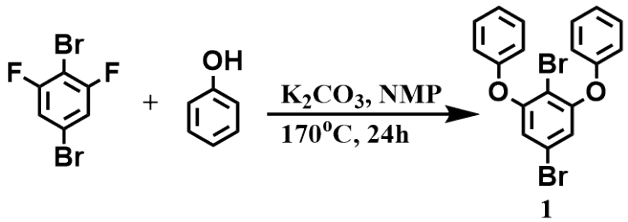

In a 500 mL two neck round bottom flask, 2,5-dibromo-1,3-difluorobenzene (5.00 g, 18.39 mmol), phenol (3.46 g, 36.76 mmol), potassium carbonate (10.17 g, 73.58 mmol) and 100 mL N-methylpyrrolidone were sequentially added, the mixture was heated to 170 °C for 24 h. After cooling to room temperature, N-methylpyrrolidone was

removed by reduced pressure distillation and then the resulting organic layer by dichloromethane, water-soluble impurities were removed by washing the remaining reactants. The crude product was obtained by filtering, decompressing the solvent. The crude product was carried out with DCM and PE (v/v =1:60) as eluents. The white solid 6.43 g was obtained by column chromatograph and the yield was 83.18%. ^{1}H NMR (400 MHz, $CDCl_3$) δ (ppm) 7.42 - 7.38 (m, 4H), 7.20 (t, *J* = 7.4 Hz, 2H), 7.06 (d, *J* = 7.5 Hz, 4H), 6.76 (s, 2H). ^{13}C NMR (126 MHz, $CDCl_3$) δ (ppm) 156.41, 155.79, 130.10, 124.52, 121.14, 119.17, 116.89, 105.86 (**Fig.S1 and Fig.S6**).

Compound 2:

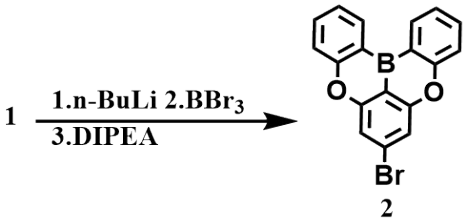

2

In a 250 mL two neck round bottom flask, the hexane solution of butyl lithium (1.97 ml, 2.4 M, 4.73 mmol) was slowly added to anhydrous o-xylene (85 mL) of **compound 1** (1.50 g, 4.29 mmol) at -30 °C. After 1 hour, the reaction system was moved to room temperature and stirred for 1.5 hours. Then slow down at -30 ºC add BBr_3 (0.49 mL, 5.16 mmol) and after 20 minutes, stir the mixture at room temperature for 3 hours. Then N, n-diisopropylethylamine (1.49 ml, 8.58 mmol) was added at 0 °C. Reaction mixture at room temperature stir for 30 minutes at 150 °C for 14 hours. After cooling to room temperature, o-xylene was removed by reduced pressure distillation. The organic layer was washed with water three times, and removed by rotary evaporation. The crude product was further purified by column chromatography, where pure petroleum ether (PE) was used as the eluent. The white solid 0.49 g was obtained by column chromatograph and the yield was 39.33%. ^{1}H NMR (400 MHz, $CDCl_3$) δ (ppm) 8.67 (dd, *J* = 7.6, 1.7 Hz, 2H), 7.72 (ddd, *J* = 8.6, 7.1, 1.7 Hz, 2H), 7.53 (d, *J* = 7.4 Hz, 2H), 7.44 – 7.38 (m, 4H). ^{13}C NMR (101 MHz, $CDCl_3$) δ (ppm) 160.28, 157.62, 134.55, 133.91, 128.41, 123.21, 118.53, 112.17 (**Fig.S2 and Fig.S7**).

Compound 3:

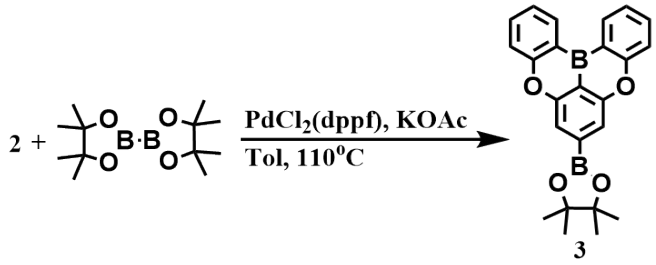

In the nitrogen atmosphere, a mixture of **compound 2** (5.00 g, 14.32 mmol), Bis(pinacolato)diboron (4.37 g, 17.19 mmol), $PdCl_2$(dppf) (0.31 g, 0.43 mmol), KOAc (7.02 g, 71.56 mmol) were dissolved in 250 ml of toluene in the round-bottom flask. Then, the reaction mixture was heated to 120 °C and stirred for 24 h. After cold to room temperature, the reaction mixture was filtered with suction, washed with dichloromethane and then removed the solvent in vacuo. The crude product was purified by silica gel column chromatography (elution with PE) to give the **compound 3** (4.71 g, 84.21%). ^{1}H NMR (400 MHz, $CDCl_3$) δ (ppm) 8.72 (dd, *J* = 7.7, 1.6 Hz, 2H), 7.74 (ddd, *J* = 8.5, 7.0, 1.7 Hz, 2H), 7.70 (s, 2H), 7.57 (d, *J* = 8.4 Hz, 2H), 7.41 (t, *J* = 7.3 Hz, 2H), 1.43 (s, 12H). ^{13}C NMR (126 MHz, $CDCl_3$) δ (ppm) 156.86, 151.64, 151.15, 140.36, 139.45, 131.07, 127.86, 117.30, 114.96, 113.79, 55.52 (**Fig.S3 and Fig. S8**).

Compound 4:

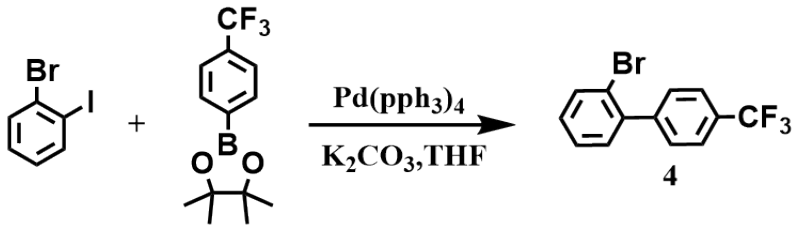

In a 200 mL two-necked, round-bottomed flask and fitted with a stirrer and a condenser tube, a mixture of 1-bromo-2-iodobenzene (1.00 g, 3.68 mmol), 4,4,5,5-tetramethyl-2-(4-(trifluoromethyl)phenyl)-1,3,2-dioxaborolane (0.96 g, 3.68 mmol), $Pd(pph_3)_4$ (254.22 mg, 0.22 mmol), K_2CO_3 (9.2 ml, 2M, 18.40 mmol) were dissolved in 30 mL of THF under anhydrous and Ar condition. The reaction was placed in a preheated oil bath at 65 ℃ for 24 h. After cold to room temperature, the reaction mixture was filtered with suction, washed with dichloromethane and then removed the solvent in vacuo. The crude product was purified by silica gel column chromatography (elution

with PE) to give the transparency liquid **compound 4** (0.41 g, 38.53%). ^{1}H NMR (400 MHz, CD_2Cl_2) δ (ppm) 7.71 (dd, *J* = 7.9, 1.3 Hz, 1H), 7.58 – 7.53 (m, 3H), 7.47 (dd, *J* = 8.0, 1.2 Hz, 1H), 7.40 (d, *J* = 8.0 Hz, 2H), 7.24 (dd, *J* = 11.1, 3.8 Hz, 1H), 7.17 (dd, *J* = 7.6, 1.5 Hz, 1H), 7.13 – 7.05 (m, 1H), 6.84 (td, *J* = 7.8, 1.3 Hz, 1H). ^{13}C NMR (101 MHz, CD_2Cl_2) δ (ppm) 144.6, 141.2, 140.3, 133.3, 132.8, 131.1, 130.2, 130.11 – 129.7, 129.72 – 129.1, 128.3, 127.65, 125.6, 125.06, 122.9, 122.33, 120.22, 101.28, 77.43, 77.11, 76.79 (**Fig.S4 and Fig.S9**).

Compound BOBTFB:

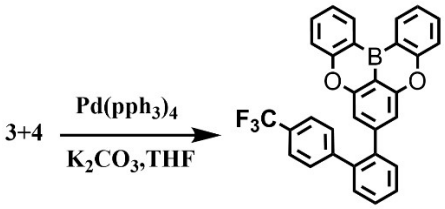

BOBTFB

Sequentially adding compounds **compound 3** (0.53 g, 1.36 mmol), **compound 4** (0.41 g, 1.36 mmol), $Pd(pph_3)_4$ (94.75 mg, 0.08 mmol), K_2CO_3 (2.72 ml, 2M, 5.44 mmol) and 10 mL THF into a 50 mL single-neck round-bottom flask, the mixture was refluxed at 65 °C for 24 hours. The mixture was cooled to room temperature, poured into water, and extracted with DCM three times. Then removed the solvent in vacuo to give the crude product. The white solid 0.21 g was obtained by column chromatograph (elution with PE) and the yield was 31.48%. ^{1}H NMR (400 MHz, CD_2Cl_2) δ (ppm) 8.62 (dd, *J* = 7.7, 1.6 Hz, 2H), 7.64 (ddd, *J* = 8.6, 7.1, 1.7 Hz, 2H), 7.52 – 7.47 (m, 2H), 7.47 – 7.45 (m, 1H), 7.44 (d, *J* = 4.1 Hz, 2H), 7.43 – 7.40 (m, 2H), 7.39 (s, 1H), 7.34 (d, *J* = 1.0 Hz, 1H), 7.32 (d, *J* = 2.9 Hz, 2H), 7.31 – 7.29 (m, 1H), 6.96 (s, 2H). ^{13}C NMR (101 MHz, $CDCl_3$) δ (ppm) 162.42, 158.93, 150.3, 146.9, 141.98, 141.07, 136.45, 135.67, 132.91, 132.65, 132.09, 130.61, 130.28, 126.89, 124.82, 120.26, 112.00, 55.94, 55.67, 55.39, 55.12, 54.85, 2.73 (**Fig.S5 and Fig.S10**).

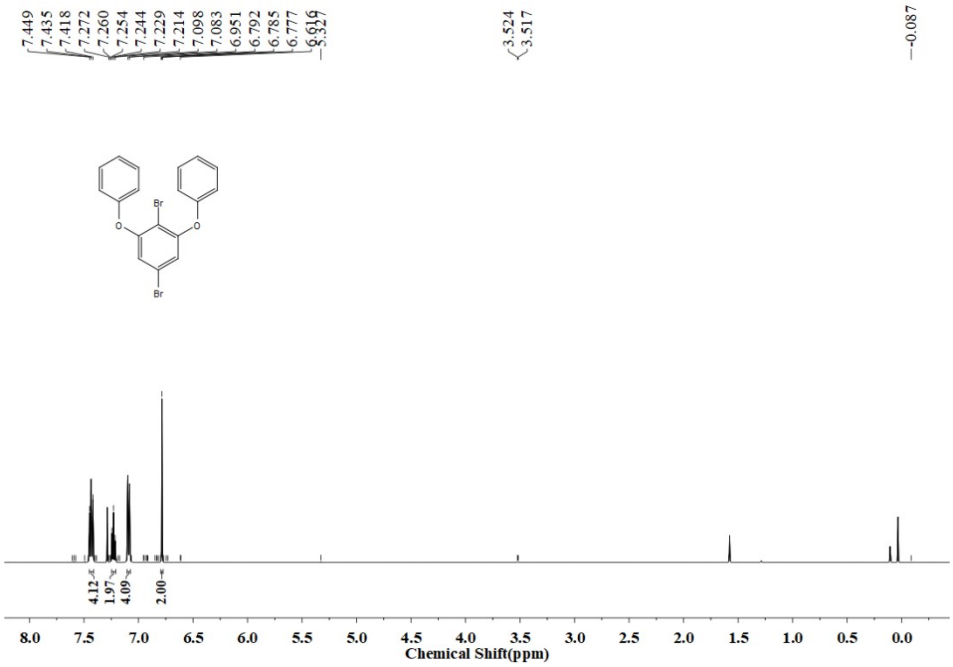

Fig.S1. [1]H NMR spectrum of compound **1**.

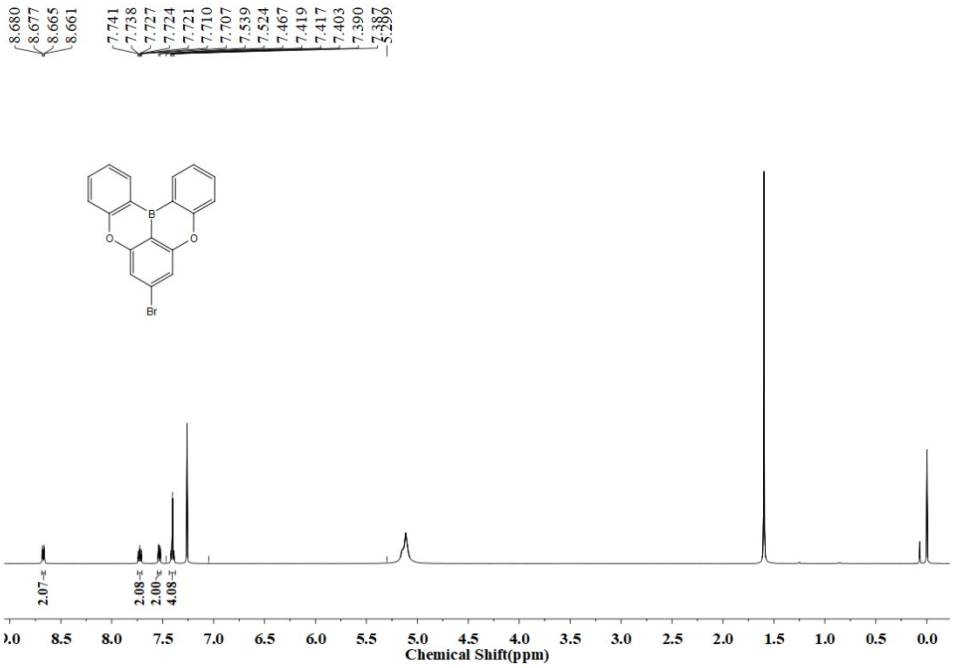

Fig.S2. [1]H NMR spectrum of compound **2**.

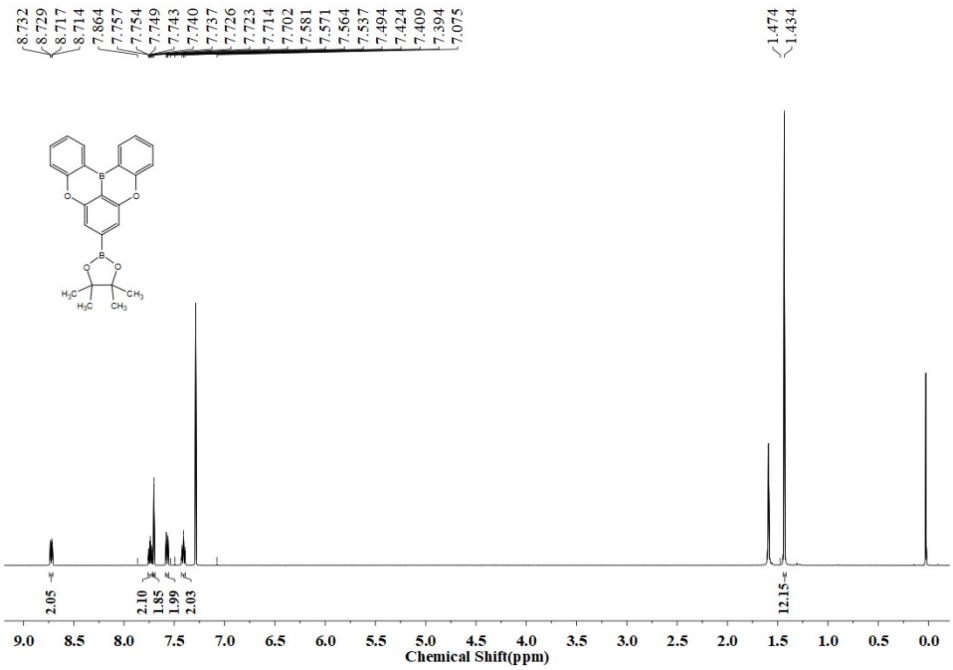

Fig.S3. [1]H NMR spectrum of compound **3**.

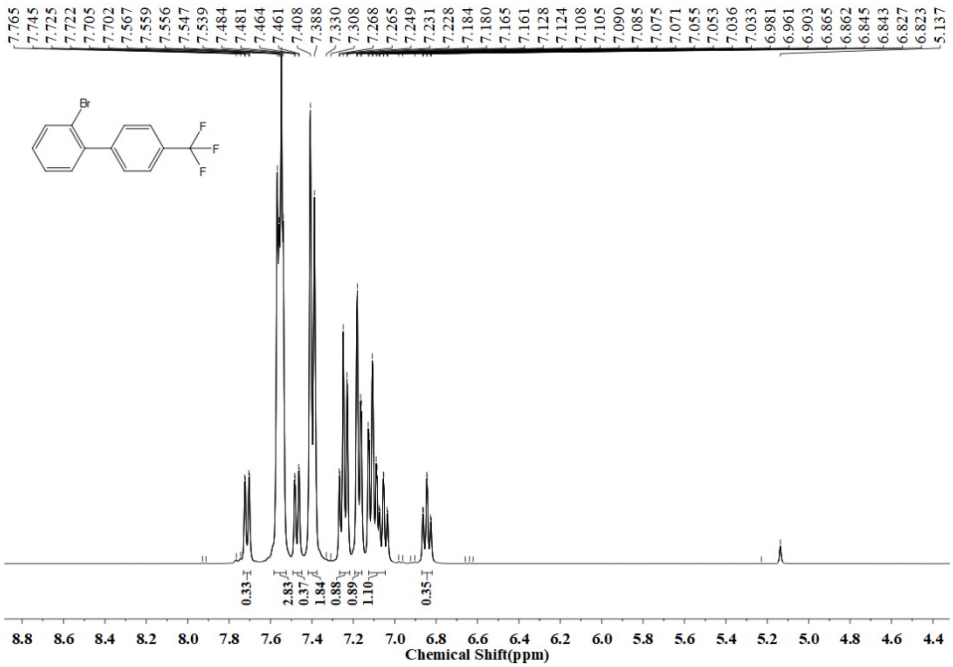

Fig.S4. [1]H NMR spectrum of compound **4**.

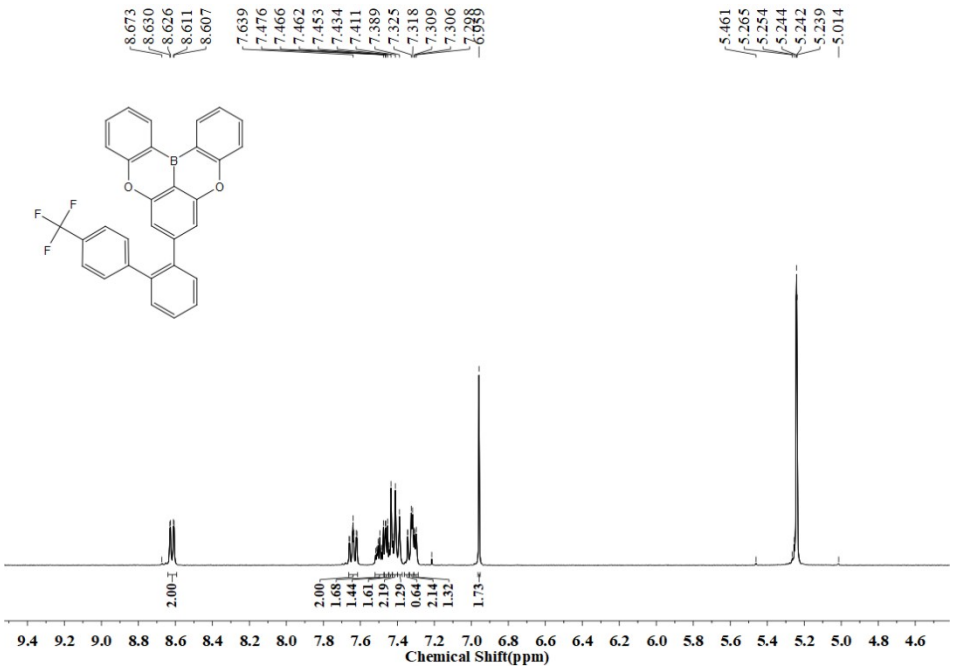

Fig.S5. ^{1}H NMR spectrum of **BOBTFB**.

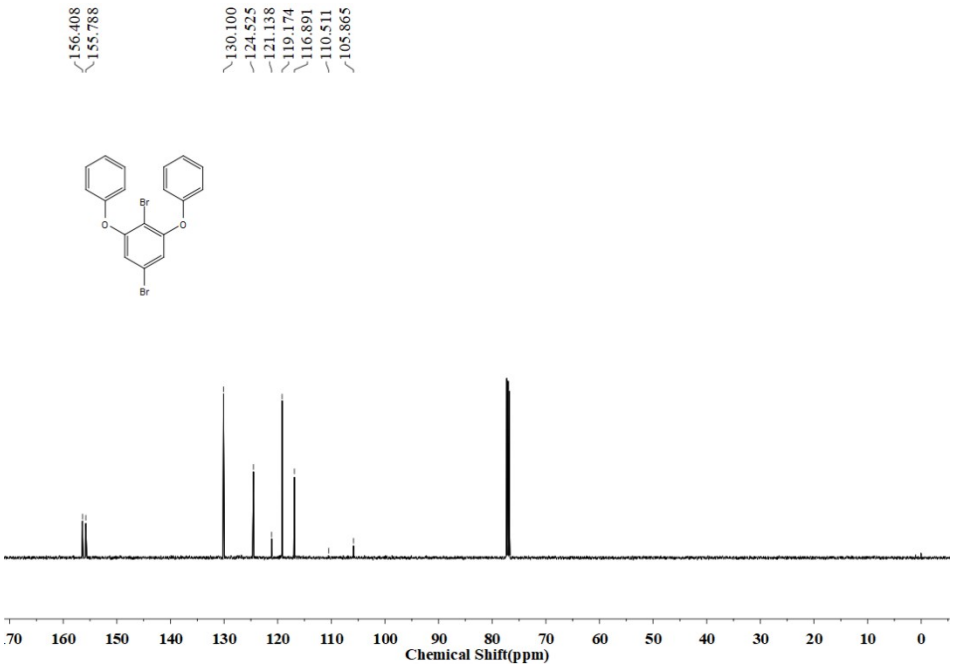

Fig.S6. ^{13}C NMR spectrum of compound **1**.

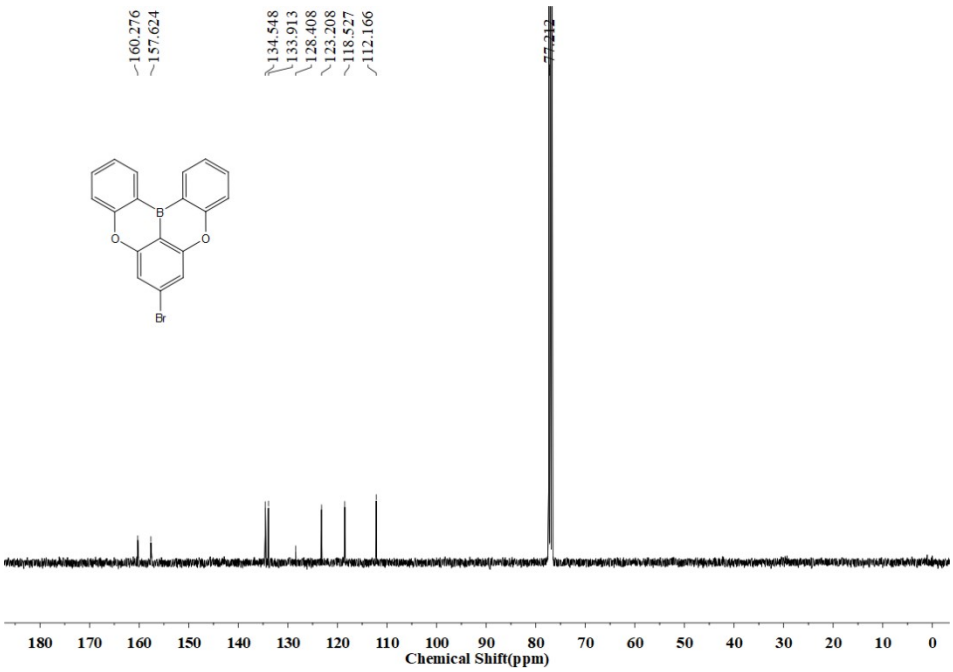

Fig.S7. ^{13}C NMR spectrum of compound **2**.

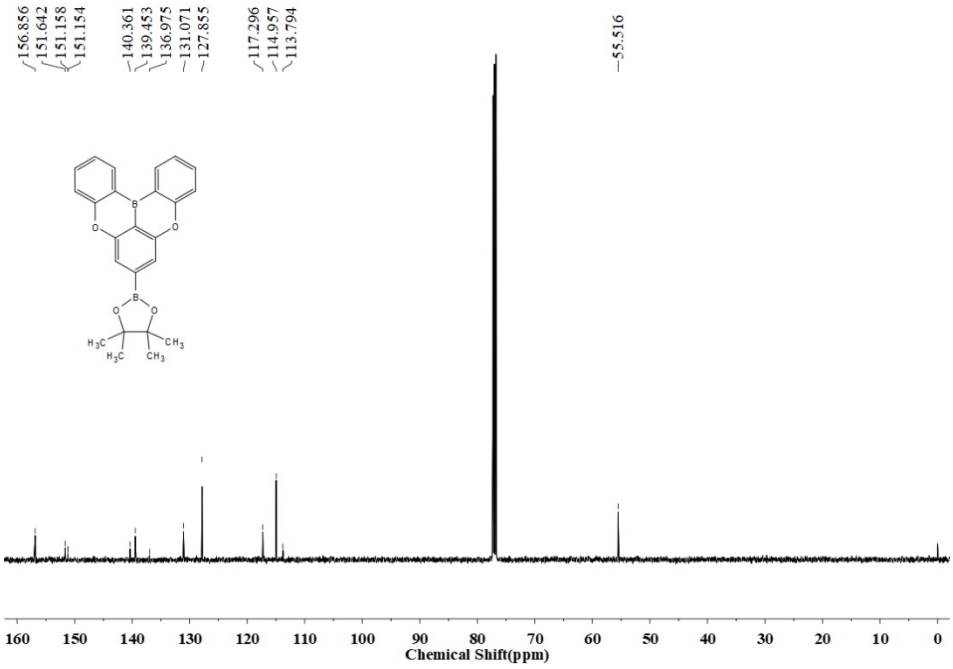

Fig.S8. ^{13}C NMR spectrum of compound **3**.

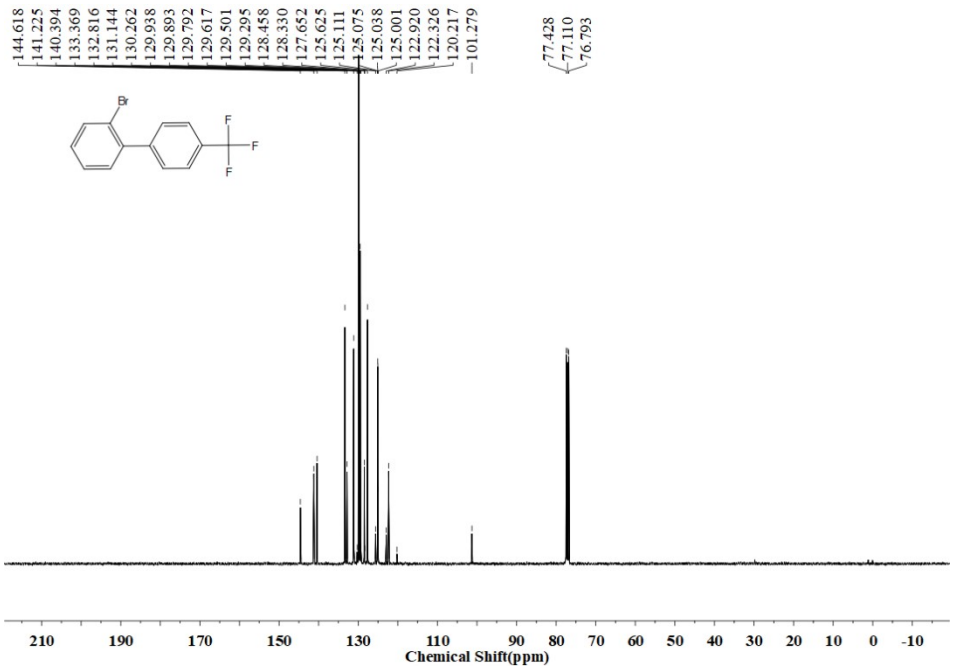

Fig.S9. ^{13}C NMR spectrum of compound **4**.

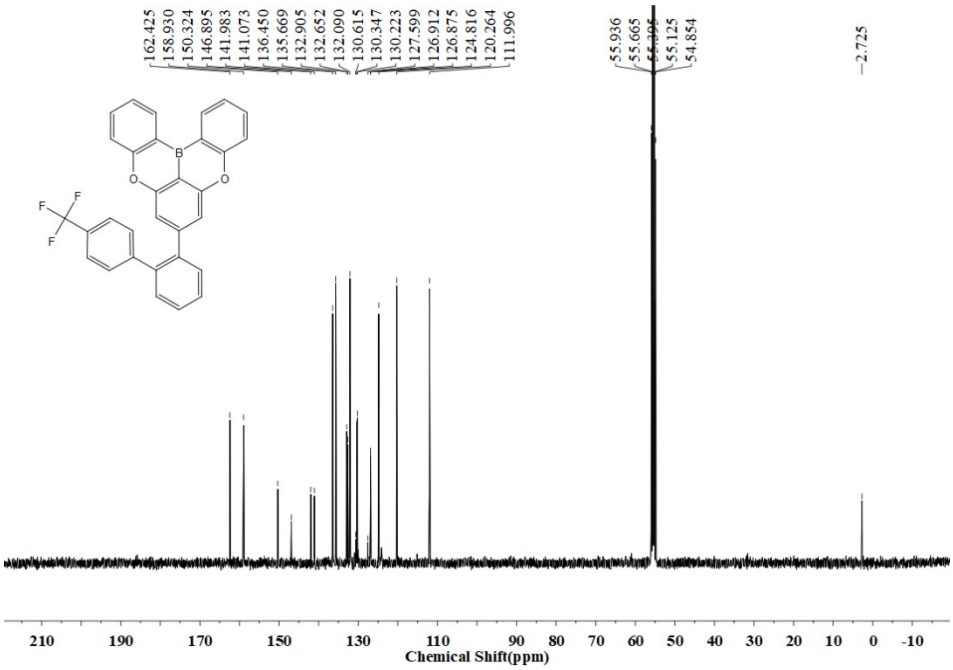

Fig.S10. ^{13}C NMR spectrum of **BOBTFB**.

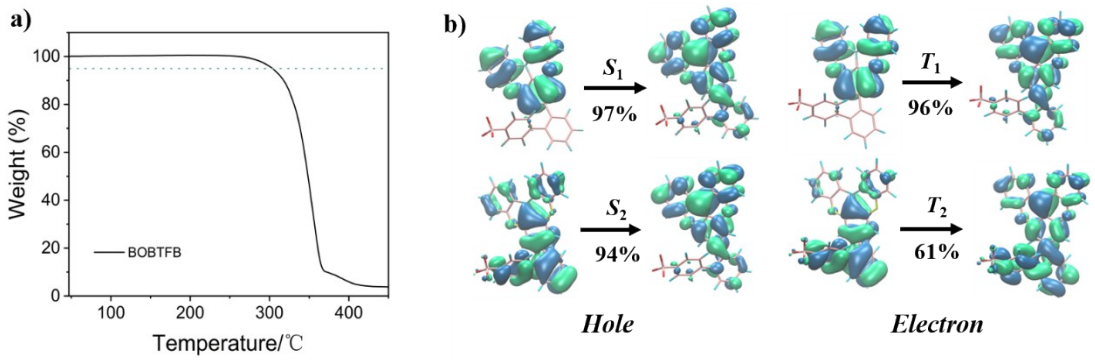

Fig.S11. a) TGA curve of BOBTFB; b) Natural transition orbits from S_0 to S_1 and T_1 of BOBTFB.

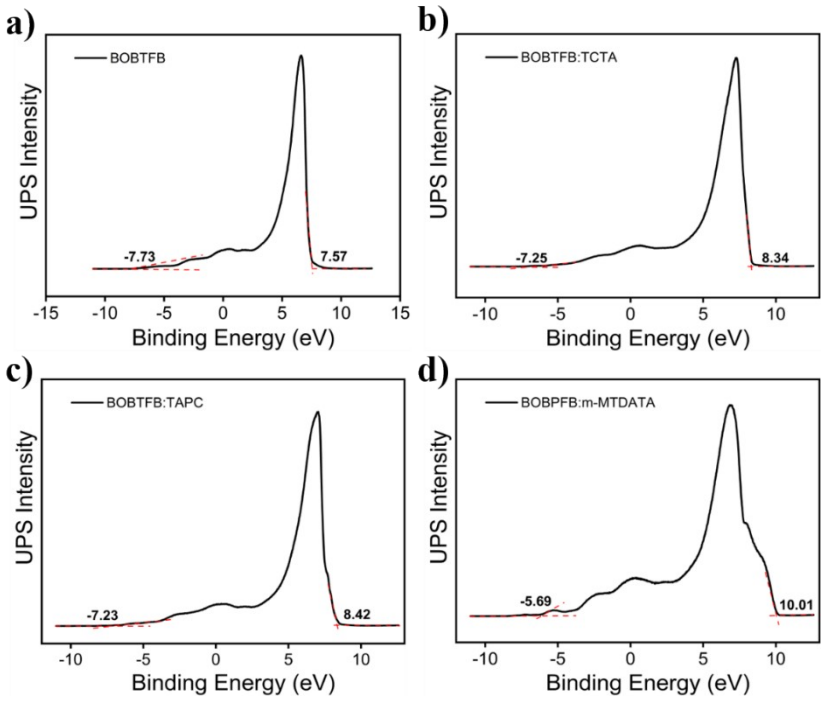

Fig.S12. Ultraviolet photeletron spectra (UPS) of a) neat film of BOBTFB, b) exciplex films of BOBTFB:TCTA (2:8) ; c) BOBTFB:TAPC (9:1) and) BOBTFB:m-MTDATA (1:9) (mass ratio), respectively.

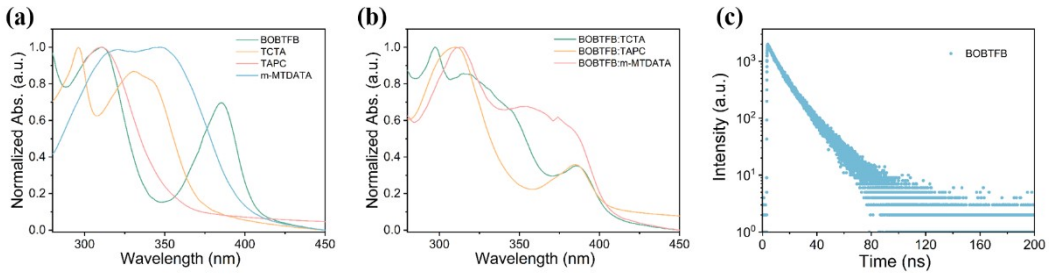

Fig.S13. a) Absorption spectra in neat films of BOBTFB, TCTA, TAPC and m-MTDATA; b) Absorption spectra of exciplex films of BOBTFB:TCTA (2:8), BOBTFB:TAPC (9:1) and c) BOBTFB:m-MTDATA (1:9) (mass ratio); c) The PL decay curve of neat film of BOBTFB at 300 K, respectively.

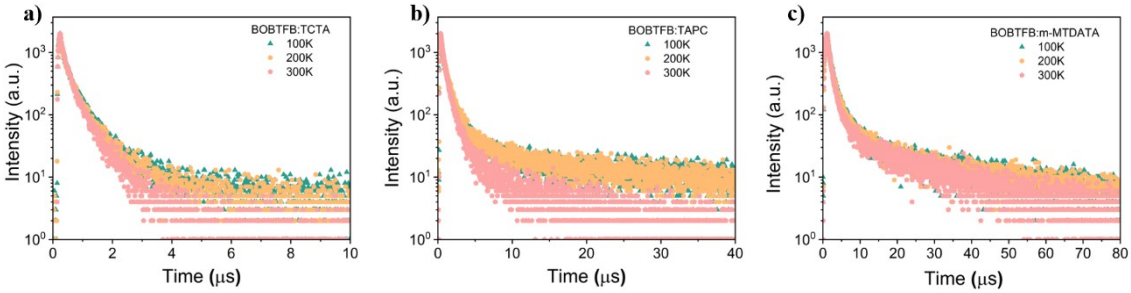

Fig.S14. The temperature-dependent transient PL decay curves of a) BOBTFB:TCTA (2:8), BOBTFB:TAPC (9:1) and c) BOBTFB:m-MTDATA (1:9) exciplex films at temperatures ranging from 100 K to 300 K.

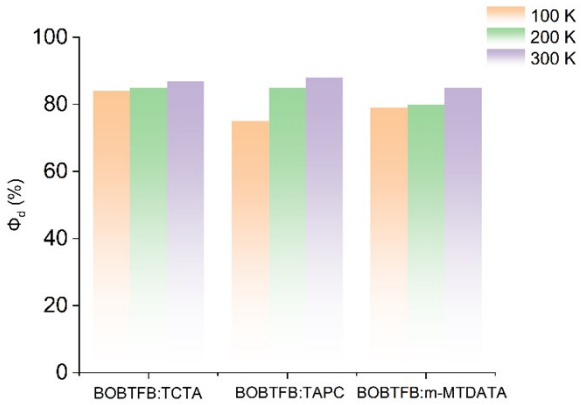

Fig.S15. Proportion of delay components of BOBTFB:TCTA (2:8), BOBTFB:TAPC (9:1) and BOBTFB:m-MTDATA (1:9) exciplex films at different temperatures.

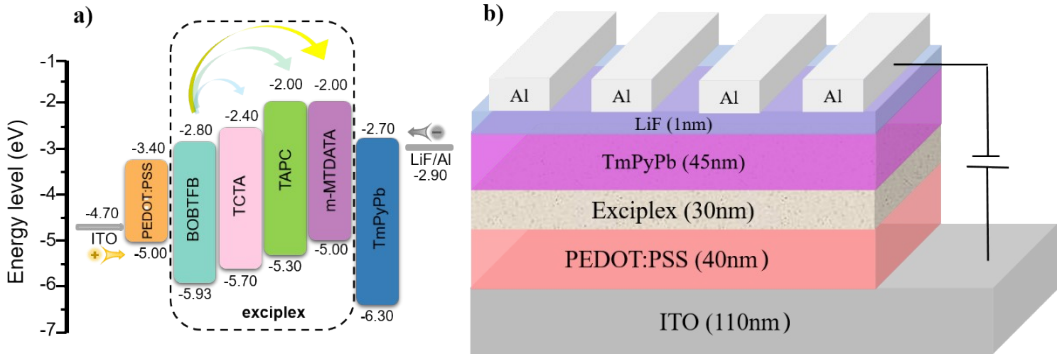

Fig.S16. a) Energy-level diagrams, (b) device structures.

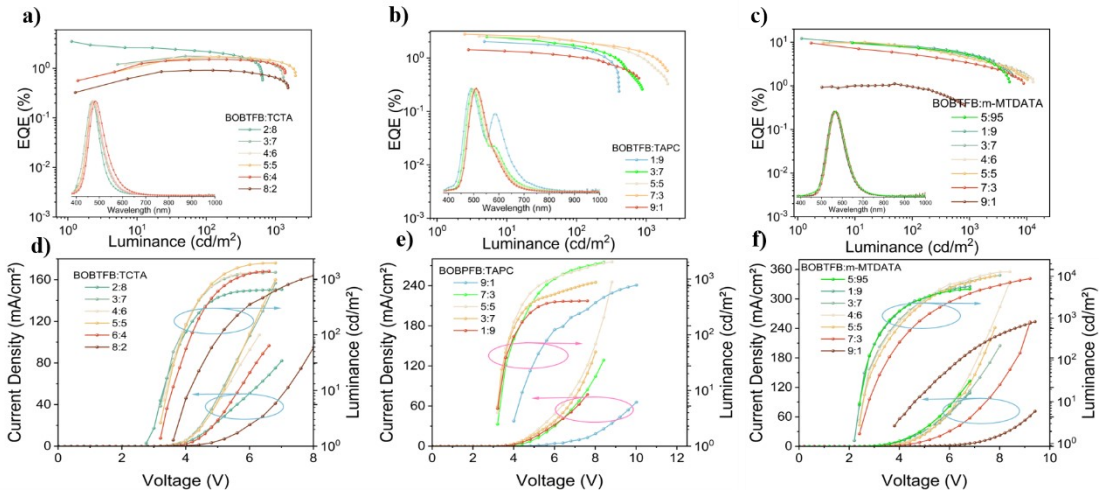

Fig.S17. (a-c) EL spectra and *EQE-L* curves and (d-f) *J-V-L* curves of different co-doped ratios of BOBTFB:TCTA, BOBTFB:TAPC and c) BOBTFB:m-MTDATA mixed films with different weight ratios, respectively.

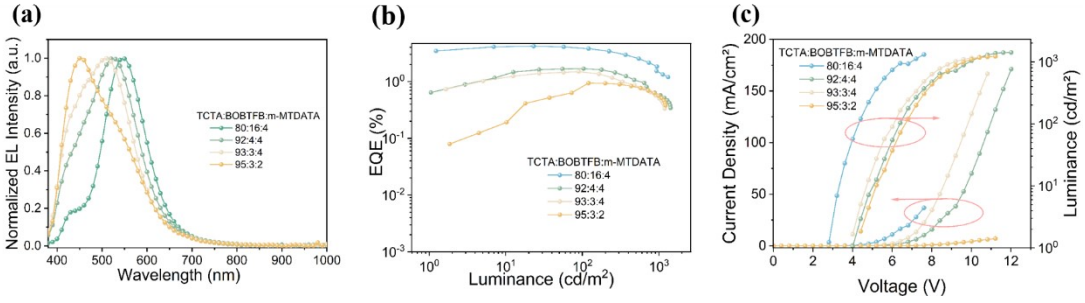

Fig.S18. (a) EL spectra, (b) *EQE-L* and (c) *J-V-L* curves of TCTA:BOBTFB:m-MTDATA mixed films with different weight ratios, respectively.

Table S1. Relevant information derived from the UPS spectra of neat BOBTFB film, and various exciplex films with different weight ratios.

films	$E_{cut\text{-}off}$ (eV)	$E_{cut\text{-}off}$ (eV)	$\Delta E_{cut\text{-}off}$ (eV)	[a)] E_{HOMO} (eV)	[b)] E_{LUMO} (eV)	E_g [c)] (eV)
BOBTFB	-7.73	7.57	15.30	-5.92	-2.75	3.17
BOBTFB:TCTA (2:8)	-7.25	8.34	15.59	-5.63	-2.61	3.02
BOBTFB:TAPC (9:1)	-7.23	8.42	15.65	-5.57	-2.57	3.00
BOBTFB:m-MTDATA (1:9)	-5.69	10.01	15.70	-5.52	-2.53	2.99

a) Calculated according to the equation $E_{HOMO,UPS} = (\Delta E_{cut\text{-}off} - 21.22)$ eV; b) $E_{LUMO} = E_{HOMO} + E_{g.}$; c) Calculated bandgap of BOBTFB from UV-vis absorption data.

Table S2. Photophysical parameters of exciplex films with different weight ratios.

Emitters (mass ratio)	τ_p/Φ_p **(ns/%)**	τ_d/Φ_d **(μs/%)**	k_p **($10^9 s^{-1}$)**	k_d **($10^6 s^{-1}$)**	k_{ISC} **($10^6 s^{-1}$)**	k_{RISC} **($10^6 s^{-1}$)**	k_r **($10^6 s^{-1}$)**	k_{nr} **($10^6 s^{-1}$)**
BOBTFB:TCTA (2:8)	25/1.4	1.0/9.47	0.04	1.00	39.4	6.71	0.57	0.90
BOBTFB:TAPC (9:1)	100/3.3	5.4/25.22	0.01	0.19	9.67	1.43	0.34	0.14
BOBTFB:m-MTDATA (1:9)	180/7.9	17.8/43.66	0.006	0.06	5.11	0.34	4.41	0.03

Table S3. The summary of the exciplexes based device performances for different doping ratios, respectively.

Emitters (mass ratio)	**doping ratios**	V_{on} **(V)**	λ_{EL} **(nm)**	EQE_{max} **(%)**	CE_{max} **(cd A^{-1})**	**CIE(x,y)**	L_{max} **(cd m^{-2})**
BOBTFB/ TCTA	2:8	2.8	470	3.49	4.80	(0.15,0.18)	650
	4:6	3.3	472	1.74	2.90	(0.16,0.20)	1314
	5:5	3.2	474	1.71	2.94	(0.16,0.24)	1944
	6:4	3.2	474	1.52	2.64	(0.16,0.25)	1377
	8:2	3.6	484	0.91	1.80	(0.18,0.31)	1518
BOBTFB/ TAPC	1:9	3.2	498	2.03	4.63	(0.33,0.38)	406
	3:7	3.2	498	2.49	6.14	(0.28,0.42)	874
	5:5	3.2	504	2.55	6.86	(0.28,0.45)	2073
	7:3	3.2	508	2.78	8.07	(0.28,0.48)	2009
	9:1	4.0	564	1.42	4.28	(0.26,0.49)	779
BOBTFB/ m-MTDATA	5:95	2.4	568	9.70	30.09	(0.44,0.51)	4967
	1:9	2.2	564	12.18	38.83	(0.44,0.52)	5733
	3:7	2.4	564	9.95	31.56	(0.44,0.52)	10550

	5:5	2.4	570	9.63	29.79	(0.45,0.51)	10260
	7:3	2.4	570	9.56	29.15	(0.45,0.51)	8803
	9:1	3.8	564	1.03	3.52	(0.43,0.53)	818

Table S4. The summary of device performances for BOBTFB:TCTA:m-MTDATA in different doping ratios.

[a]Emitters (mass ratios)	V_{on} (V)	CRI	EQE_{max} (%)	CE_{max} (cd A^{-1})	CIE (x,y)	L_{max} (cd m^{-2})
16:80:4	2.8	75	4.20	14.20	(0.34,0.48)	1316
4:92:4	4.0	80	1.69	5.09	(0.26,0.38)	1419
3:93:4	4.0	82	1.49	4.06	(0.23,0.33)	1191
3:95:2	4.4	84	0.94	1.03	(0.23,0.27)	1225

a) BOBTFB:TCTA:m-MTDATA (mass ratio).

Table S5. Crystal data of the compound BOBTFB (This crystal was obtained via slow evaporation of a CH_2Cl_2/methanol (v:v/1:1) mixture solvent).

Identification code	BOBTFB
Empirical formula	$C_{31}H_{18}BF_3O_2$
Formula weight	490.26
Temperature/K	170
Crystal system	monoclinic
Space group	$P2_1/c$
a/Å	7.1623(2)
b/Å	18.0515(8)
c/Å	17.7717(7)
α/°	90

β/°	91.3520(10)
γ/°	90
Volume/Å^3	2297.07(15)
Z	4
ρ_{calc}g/cm^3	1.418
μ/mm^{-1}	0.103
F(000)	1008.0
Crystal size/mm^3	0.15 × 0.09 × 0.05
Radiation	MoKα (λ = 0.71073)
2Θ range for data collection/°	4.512 to 52.86
Index ranges	-8 ≤ h ≤ 8, -22 ≤ k ≤ 22, -22 ≤ l ≤ 22
Reflections collected	21212
Independent reflections	4614 [Rint = 0.0940, Rsigma = 0.0777]
Data/restraints/parameters	4614/0/334
Goodness-of-fit on F^2	1.003
Final R indexes [I>=2σ (I)]	R_1 = 0.0570, wR_2 = 0.1407
Final R indexes [all data]	R_1 = 0.1102 wR_2 = 0.1829
Largest diff. peak/hole / e Å^{-3}	0.25/-0.30